Regenerability of Antibacterial Activity of Interpenetrating Polymeric *N*-Halamine and Poly(ethylene terephthalate)

Nan Zhao,[1] George G. Zhanel,[2] Song Liu[1]

[1]*Department of Textile Sciences, Faculty of Human Ecology, University of Manitoba, Winnipeg, Manitoba, Canada*
[2]*Department of Medical Microbiology, Faculty of Medicine, University of Manitoba, Winnipeg, Manitoba, Canada*

Received 19 June 2010; accepted 16 August 2010
DOI 10.1002/app.33208
Published online 20 October 2010 in Wiley Online Library (wileyonlinelibrary.com).

ABSTRACT: Effective antibacterial modification of poly(ethylene terephthalate) (PET) was achieved by forming a surface thermoplastic semi-interpenetrating network of polyacrylamide (PAM) and PET, followed by converting the immobilized amides to *N*-halamine. The regenerability of *N*-halamine on PAM-modified PET was significantly influenced by the cross-linkers used to form the network. Through Fourier transform infrared spectroscopy and nitrogen content analysis of the materials for up to 29 regeneration cycles, it was found that breaking down of the PAM network in chlorination accounted for the loss of regenerability. The relationship between antibacterial efficacy and *N*-halamine concentration was also studied. Compared with *N*,*N*′-methylenebisacrylamide and 2-ethyleneglycol diacrylate, cross-linker divinylbenzene can generate more durable PAM network. After 29 regeneration cycles, the PAM-divinylbenzene network-modified PET was still able to provide 100% reduction of healthcare-associated methicillin-resistant *Staphylococcus aureus* in 20 min contact. © 2010 Wiley Periodicals, Inc. J Appl Polym Sci 120: 611–622, 2011

Key words: surface modification; cross-linking; interpenetrating network; radical polymerization; FTIR

INTRODUCTION

Thousands of tons of waste are generated worldwide in hospitals each day. Depending on region and hospital, the weight percentage of textiles in medical waste ranges from 11% to 26%.[1–4] A good strategy to reduce waste is reuse. Textiles are among the materials in health-care settings, which have reduction, recycling, and reuse potential. Reusable medical textiles have received attention because of their advantage of offering more efficient protection besides reducing wastes and costs.[5] Compared with natural fibers, synthetic fibers such as nylon, poly(ethylene terephthalate) (PET), and polypropylene are better fibers for reusable surgical gowns, protective drapes, or cubicle curtains because of their superior chemical and mechanical durability. However, PET is susceptible to contamination of many microorganisms including bacteria, viruses, and spores,[6–9] and the contaminated PET can serve as one of the major sources of infectious diseases. To decrease the possibility of cross-infection, it is necessary to introduce antibacterial property or function to PET surface.

However, modification of PET is challenging because of its chemically inert characteristics, high crystallinity, and hydrophobicity. Radical grafting polymerization, a chemical modification method, seems to be a desirable process for modification because even chemically inert polymers such as PET can be surface modified to introduce new functions without compromising their bulk properties.[10–17] In recent years, the formation of surface interpenetrating network (IPN) polymers has emerged as a viable alternative to synthetic grafting techniques in upgrading the properties of chemically inert polymers like PET.[18,19] Specifically, acrylamide (AM), divinyl cross-linker *N*,*N*′-methylenebisacrylamide (MBA), and photoinitiator benzophenone (BP) diffuse into the swollen surface of PET and polymerize *in situ* to form a thermoplastic semi-IPN. It is named as such because the substrate thermoplastic PET is physically cross-linked, whereas the immobilized functional polymer is chemically cross-linked to physically interlock with the substrate polymer. Thermoplastic IPN involves only physical cross-links (crystalline areas serve as cross-linking point); in semi-IPN, one linear or branched polymer is blended with another chemically cross-linked polymer network. Neither of the two definitions fits this situation; thus, two descriptors "thermoplastic" and "semi" are combined to reflect the similarity between the synthesis of this structure and the other two IPNs. The immobilized polyacrylamide (PAM) is durable on Soxhlet extraction with distilled

Correspondence to: S. Liu (lius0@cc.umanitoba.ca).
Contract grant sponsors: Natural Sciences and Engineering Research Council of Canada (NSERC) Discovery, Manitoba Health Research Council (MHRC) Establishment, Manitoba Medical Science Foundation (MMSF), University of Manitoba.

(DI) water for 72 hr, and with methanol for additional 24 hr. Advantages of this new technique include the absence of damage to the base substrate, achievable high efficiencies and densities, and mild reaction conditions.

The immobilized amide can be converted to acyclic *N*-halamine, which has been disclosed by several investigators as an effective biocide.[12,20–26] However, it was found that the immobilized amide structure was lost after several chlorination–quench cycles leading to decreased amount of *N*-halamine and compromised antimicrobial efficacy. This will hinder its application as reusable antibacterial textile material. It is inferred that the hydrolysis of the cross-linker MBA during chlorination causes the damage of the thermoplastic semi-IPN. The hydrolytic durability of the formed IPN is attributed to the chemical durability of the cross-linking structure. It is expected that forming the thermoplastic semi-IPN with a nonhydrolyzable cross-linker will impart the *N*-halamine-modified PET with a better regenerable antimicrobial performance. Therefore, the aim of this article is to report the findings of a systematic study of the effects of the type of the cross-linker on the durability of the IPN, which is closely related to the regenerability of biocidal moiety, *N*-halamine. In this study, we investigated regenerability of the antibacterial performance of surface thermoplastic IPN between PAM and PET with three different cross-linkers: MBA, divinylbenzene (DVB), and 2-ethyleneglycol diacrylate (EGDA) (PAM-PET-M, PAM-PET-D, and PAM-PET-E), and studied the mechanisms accounting for the loss of *N*-halamine regenerability.

EXPERIMENTAL

Materials

PET-woven fabric No. 777H was purchased from Test Fabrics Inc. (West Pittiston, PA). AM, DVB, EGDA, MBA, and some other reagents were purchased from Aldrich (St. Louis, MO). Cross-linker DVB with 1000 ppm inhibitor 4-*tert*-butylcatechol was washed four times with an equal volume of an aqueous solution of 10% sodium hydroxide, followed by four rinses with deionized water, to remove the inhibitor.

Modification of PET

PET fabrics were surface-modified with PAM by forming an IPN. Briefly, a PET round fabric swatch with a diameter of 4.25 in. was first swollen in methanol solution of BP, AM, and cross-linker at 40°C for 30 min (duration of swelling). Excess solution was dripped off from the specimen and absorbed by the filter paper for 5 sec to achieve around 120% pickup of the solution. The fabric was then exposed to ultraviolet (UV) irradiation (365 nm) for 60 min. After polymerization, the PET sample was extracted with DI water in a Soxhlet extractor for 24 hr, dried at 105°C, and stored in a desiccator (humidity <20%) for 48 hr to reach constant weight.

TABLE I
Monomers and Polymers

AM	Acrylamide
MBA	*N*,*N*′-Methylene bisacrylamide
DVB	Mixture of divinylbenzene isomers
EGDA	2-Ethyleneglycol diacrylate
PET	Poly(ethylene terephthalate)
PAM	Polyacrylamide
PAM-PET	
PAM-PET-M	Thermoplastic semi-IPN between PET and PAM, cross-linker: MBA
PAM-PET-D	Thermoplastic semi-IPN between PET and PAM, cross-linker: DVB
PAM-PET-E	Thermoplastic semi-IPN between PET and PAM, cross-linker: EGDA

The immobilization percentage (IP) was calculated from the following equation:

$$\text{Immobilization percentage (IP)} = (W_2 - W_1)/W_1 \times 100 \quad (1)$$

where W_1 and W_2 are the weights of the pristine and the modified PET samples, respectively. The modified PET fabrics are specified in Table I.

N-Halamine regenerability study

To assess the regenerability of *N*-halamine on the PAM-PET samples, they were treated with "chlorination–quench–regeneration" cycles. The immobilized polyamide was converted to *N*-halamine structure by chlorinating the PAM-PET fabrics in sodium hypochlorite solution (1500 ppm available chlorine) at room temperature for 30 min. The liquid-to-fabric (liquor) ratio was 30 : 1 (w/w). The fabrics were then rinsed thoroughly with an excess amount of DI water and air-dried for 24 hr. An iodometric titration method was adopted to quantify the active chlorine on the samples right after the air-dry process. About 0.26–0.27 g of the sample fabric was cut into small pieces and added into 25 mL of 0.001*N* sodium thiosulfate standard solution. After 30 min of shaking, the excess amount of sodium thiosulfate in the mixture was titrated with 0.001*N* iodine standard solution by monitoring millivolt changes with a redox electrode (platinum Ag/AgCl). The active chlorine concentration of the modified PET samples was then calculated from the following equation:

$$\text{Active chlorine concentration } [Cl^+] \text{ (ppm)} = 35.45 \times (V_1 - V_2) \times N \times 1000/(2 \times W) \quad (2)$$

where V_1 and V_2 are the volumes (mL) of the iodine solution consumed in titrations of blank sodium thiosulfate solution and that with PET sample in, respectively, N is the normality of iodine solution, and W is the weight of the samples in grams. After titration, the fabrics were rinsed thoroughly with copious amounts of DI water and dried at 105°C for 2 hr. The active chlorine was quenched in the titration process, which means that N-Cl was changed back to N-H. Immediately after the quenching, rinsing, and drying, the *N*-halamine structure was regenerated from amide with another chlorination process. Conversion ratio of N-H to N-Cl can be calculated from the following equation:

$$\text{Conversion ratio (\%)} = [\text{Cl}] \times M(\text{AM})/(\text{IP} \times M(\text{Cl}) \times 100) \quad (3)$$

where M(AM) and M(Cl) are the molecular weight of the AM and chlorine respectively, and IP refers to the immobilization percentage of PAM.

Characterization

Fourier transform infrared spectroscopy (FTIR) spectra were taken on a Nicolet iS10 spectrometer (Thermo Fisher Scientific Inc.) using KBr pellets. Carbon, hydrogen, and nitrogen contents on PET samples were quantified after elemental analysis at the Guelph Chemical Laboratories Ltd.

Titration of surface COOH group

About 0.2 g of PET sample was immersed into 10 mL ethanol solution of thionine acetate (A_1 and V_1) (0.5 mg/mL), and the reaction solution was stirred at room temperature for 10 hr. The sample was removed, washed four times with ethanol, all solutions were combined (A_2 and V_2), and UV adsorption of which was then recorded (wavelength = 605 nm and ε = 54,300). The amount of carboxylic acid groups on unit weight of PET sample can be calculated according to the following equation:

$$[\text{COOH}] = (A_1 \times V_1 - A_2 \times V_2)/(\varepsilon \times b \times W) \quad (4)$$

where A_1 and A_2 are the UV absorptions of the original thionine acetate solution and the combined solution after test, V_1 and V_2 are the volume of the original thionine acetate solution (10 mL) and the combined solution after test, b is the path length (1 cm), and W is the weight of the tested PET sample.

Swelling capacity

Before the test, PET samples were stored in desiccators for 48 hr to reach constant weight (W_2). Then, 0.2 g of the equilibrated PET sample was immersed in 100 mL of DI water. After 1 hr of immersion, the sample was taken out and placed in a centrifuge tube with the bottom half filled with cotton fibers to retain the spin off solution. The centrifugation was carried out at 1200 rpm for 15 min. The weight was recorded immediately after the centrifugation (W_1). The swelling ratio is expressed as the ratio between the weight of the wet sample and that of the dry sample, i.e.,W_1/W_2. The swelling ratio of immobilized PAM network could be calculated from the ratio of PAM-PET and PET pristine.

$$\text{Swelling ratio of immobilized PAM} = (W_1/W_2 \times (1 + \text{IP}) - W_0'/W_0)/\text{IP} \quad (5)$$

where W_0' and W_0 are the weight of the wet pristine PET and dry pristine PET, respectively, and IP is the immobilization percentage of the studied PAM-PET fabric.

Antibacterial assessment

Antibacterial properties of the modified PET samples were examined according to a modified American Association of Textile Chemist and Colorists (AATCC) test method 100-2004 against a clinical isolate of healthcare-associated methicillin-resistant *Staphylococcus aureus* (HA-MRSA) isolate #70527 (obtained from the CANWARD study assessing antimicrobial resistance in Canadian hospitals; www.canr.ca). The fabrics were cut into two small pieces (4.8 cm in diameter), and one piece of fabrics was put in a sterilized container. One hundred microliters of an aqueous suspension containing 10^5–10^6 colony forming units (CFU)/mL of MRSA was placed onto the surface of the fabric. The inoculum on the fabric was then covered with another piece of the same fabric. To ensure sufficient contact, a sterilized 100-mL beaker was place onto the top of the fabrics. After varying contact times, the inoculated samples were placed into 10 mL of 1.0% sodium thiosulfate aqueous solution to neutralize any active chlorine. The mixture then went through vigorous shaking for 2 min and ultrasonic treatment for 5 min. An aliquot of the solution was removed from the mixture and then serially diluted, and 100 μL of each dilution was placed onto a nutrient agar plate. The same procedure was applied to both the bleached unmodified and modified but unbleached PET fabrics as controls. Viable bacterial colonies on the agar plates were counted after incubation at 37°C for 18 hr. Bacterial reduction is reported according to the following equation:

$$\text{Percentage reduction of bacteria (\%)} = (A - B)/A \times 100 \quad (6)$$

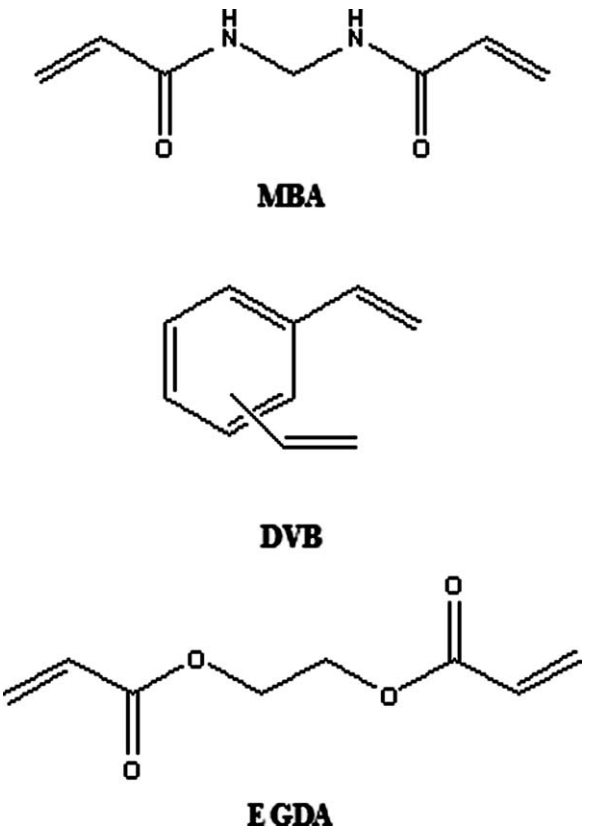

Scheme 1 Structure of the three cross-linkers (MBA, DVB, and EGDA).

where A is the number of bacteria counted from the control fabric, and B is the number of bacteria counted from modified fabric.

The bottom piece of fabric was also further investigated by leaving it on an agar and culturing for 48 hr at 37°C. Before placement of the fabric on the agar, the fabric was also pressed onto the agar five times at different parts using a sterile 100-mL beaker.

RESULTS AND DISCUSSION

Immobilization of PAM on PET with different cross-linkers

Vinyl monomer AM was copolymerized, respectively, with MBA, DVB, and EGDA (structure of which are shown in Scheme 1) in methanol-swollen PET to form a thermoplastic semi-IPN.[18] PET fabric was soaked in methanol solution of monomer AM, cross-linker (MBA, DVB, or EGDA), and photoinitiator BP at 40°C for 30 min, and, then, the excess solution was allowed to drip off and then absorbed with filter paper for 5 sec before exposing the fabric to 365 nm UV irradiation. After 1 hr irradiation, the modified PET fabric was Soxhlet extracted by DI water for 24 hr to remove unreacted monomers and unattached polymers. With all the three cross-linkers MBA, DVB, and EGDA, PAM could be efficiently immobilized on PET surface by forming the thermoplastic semi-IPN confirmed by the FTIR spectra (Fig. 1). All the modified PET fabrics are specified in Table I.

Figure 1 shows four FTIR spectra. Spectrum (a) is a result of subtracting the FTIR spectrum of pristine PET from that of PAM-PET-M spectrum (b) is a subtracted FTIR spectrum between PAM-PET-D and pristine PET; and spectrum (c) is the subtracted FTIR spectrum between PAM-PET-E and pristine PET. All three spectra show the characteristic amide I peak of PAM in the range of 1656–1661 cm^{-1}. Spectra (a) and (b) show peaks at 3427/3337 and 3203/3199 cm^{-1} corresponding to symmetric and asymmetric stretching of N—H in —C(O)NH_2. Characteristic amide I and II peaks of PAM locate at 1656/1661 and 1609 cm^{-1}, respectively. Compared with spectrum (b), the red shift of N—H stretching from 3337 to 3427 cm^{-1} and the additional medium peak at 1534 cm^{-1} on spectra (a) are due to the —NH—CO— structure of the immobilized cross-linker MBA in PAM-PET-M. Because of the high hygroscopicity of PAM-PET-E, even after long-term drying, there was still trace amount of water in the sample. The broad peak from 3100 to 3600 cm^{-1} originating from water obscures that of amide peaks in the region.

As shown in Table II, the IPs of PAM-PET-D and PAM-PET-E are much lower than that of PAM-PET-M. This is majorly due to the different reactivity ratios of DVB, EGDA, and MBA in copolymerization with AM. In copolymerization, the reactivity ratios r_1 and r_2 of two comonomers are defined as: $r_1 = k_{11}/k_{12}$ and $r_2 = k_{22}/k_{21}$, where kij is the rate constant of the reaction between growing polymer chain with monomer i unit radical and monomer j. As reported by Baselga et al.,[27] in the chain cross-linking copolymerization of AM and MBA in water, the reactivity ratio of them are 0.57 and 3.36, respectively. Although the reactivity ratios of AM and DVB (or AM and EGDA) have not been reported yet, we could predict the network buildup system through similar studies done by other researchers. It was found out that the reactivity ratios of AM and styrene in ethanol are 0.30 and 1.44.[28] The reactivity ratios of trifunctional cross-linker trimethylolpropane triacrylate and acrylic acid in radical polymerization were reported as 0.77 and 3.6, respectively.[29] Then, we can predict that, in the copolymerization of AM and DVB, the reactivity of DVB is much higher than AM, and AM radical prefers to react with DVB. As reported, the propagation rate constant of AM and styrene are 15.8×10^3 L mol^{-1} s^{-1} and 145 L mol^{-1} s^{-1}, respectively.[30,31] The reactivity of styrene radical is significantly smaller than AM radical. Because of the high reactivity of DVB monomer, it tends to participate in the polymerization and conversed to a quite stable radical, which will retard the polymerization of AM. As a result, the polymerization of

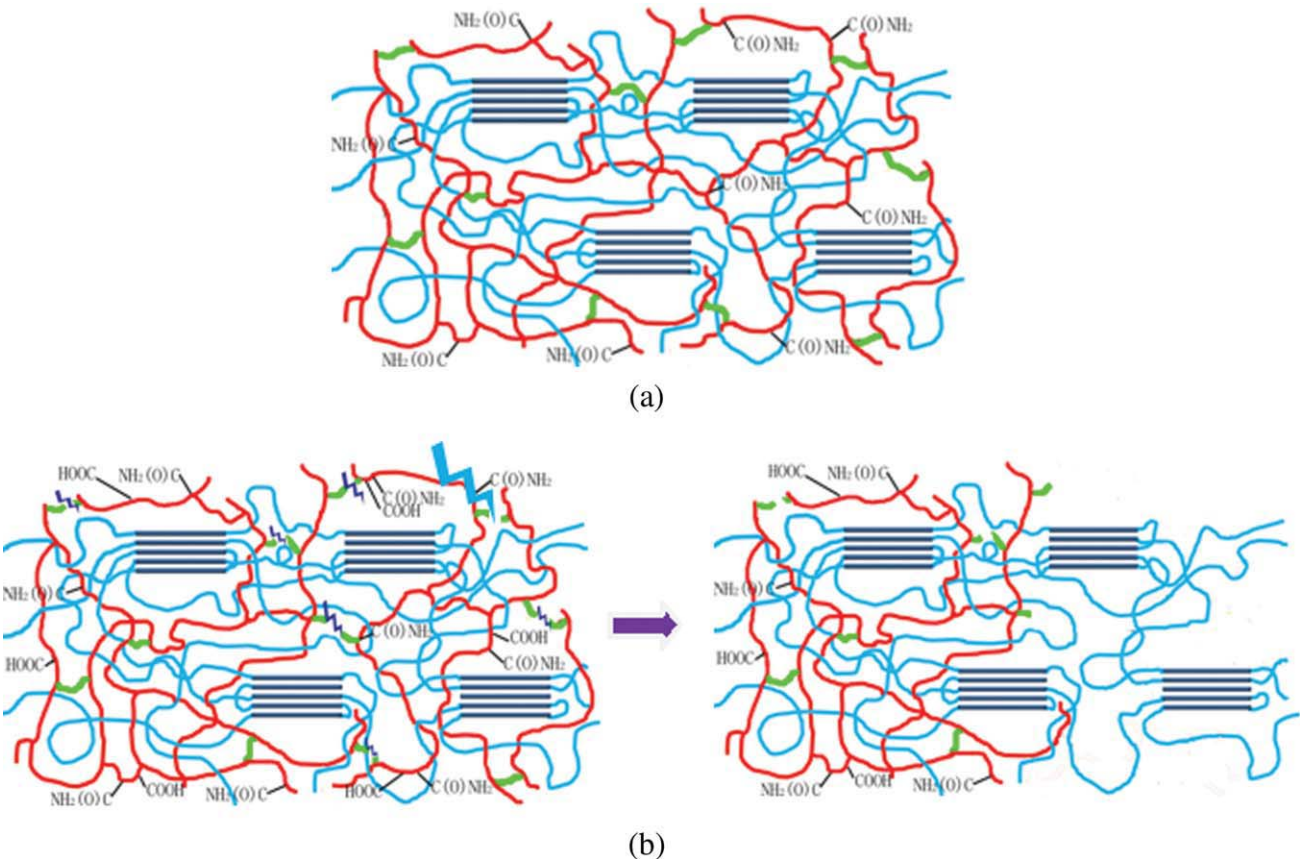

Scheme 2 Schematic diagram of the mechanism of thermoplastic semi-IPN disintegration. Blue lines represent semicrystalline polymer network. Red lines represent cross-linked poly(acrylamide). Green lines represent linkage formed by cross-linker MBA. (a) Thermoplastic semi-IPN of PAM-PET-M. (b) Loss of the network scaffold as a result of the hydrolysis of cross-linker MBA in the network. [Color figure can be viewed in the online issue, which is available at wileyonlinelibrary.com.]

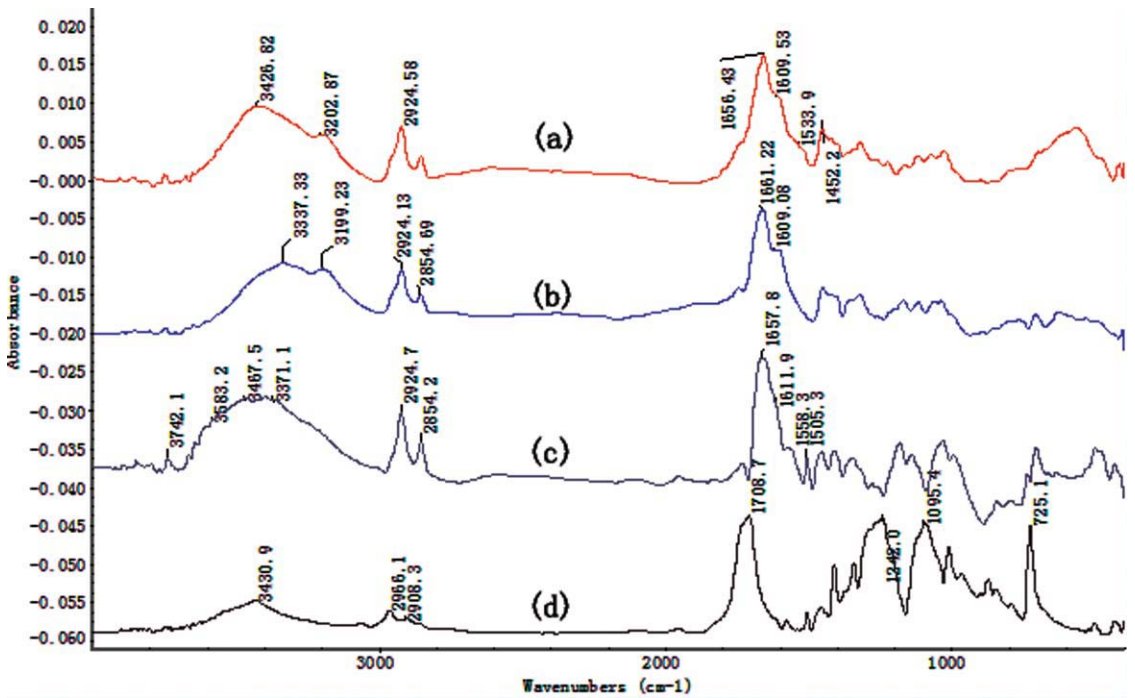

Figure 1 Subtracted FTIR spectra between (a) PAM-PET-M and pristine PET, (b) PAM-PET-D and pristine PET, (c) PAM-PET-E and pristine PET, and (d) FTIR spectra of PET pristine. [Color figure can be viewed in the online issue, which is available at wileyonlinelibrary.com.]

TABLE II
The Immobilization Percentages and Active Chlorine Concentration of the Modified PET Fabrics

Sample	Immobilization percentage (IP)	[Cl][a] (ppm)	Conversion ratio (%)
PAM-PET-M	13.9	1373	1.98
PAM-PET-D	5.8	1047	3.61
PAM-PET-E	6.2	794	2.56

AM concentration 3 mol/L, cross-linker/monomer ratio 1.5%, and BP 0.055 mol/L.
[a] Available chlorine 1500 ppm, bleached for 20 min.

AM could be hindered by DVB, and the number of successful interlocked polymer chains in PAM-PET-D is markedly smaller than that in PAM-PET-M during the given reaction time (1 hr). This would be the major reason for the smaller IP of PAM-PET-D. In addition, the segmental diffusion could also influence the network formation in the copolymerization. The polymerization of EGDA and AM could show similar phenomenon with MBA and AM, considering the similar reactivity ratios. In the previous study of copolymerization of AM with cross-linkers EGDA or MBA, it is reported that the cross-linking density of the formed hydrogel is different even starting with the same monomer and cross-linker concentrations. The hydrogel cross-linked with EGDA has lower cross-linking density and shows higher swelling capacity.[29] Lower cross-linking density of PAM-*co*-PEGDA system generates less successfully interlocked polymer chains, leading to lower IP.

Regenerability of *N*-halamine on the modified PET fabrics

The immobilized PAM on PET fabrics can be conveniently converted to acyclic *N*-halamine, which has been confirmed as a biocide demonstrating potent antibacterial activities. *N*-Halamine is favored as an antibacterial agent primarily because of its potent antibacterial activity and regenerability. Thus, we studied the regenerability of PAM-PET for 29 regeneration cycles.

In the regenerability test, the sample was treated with "chlorination–quench–chlorination" cycles. The amide-modified samples were converted to halamine structures by immersing the samples in a diluted chlorine bleach solution (1500 ppm available chlorine) at room temperature for 30 min. The active chlorine was quenched in the titration process, which was used to quantify the active chorine concentration on PAM-PET. The *N*-halamine structure could be regenerated from amide with another chlorination process.

The active chlorine contents on PAM-PET-M, PAM-PET-D, and PAM-PET-E fabrics are plotted versus the regeneration cycles in Figure 2. With all these three cross-linkers, the achieved active chlorine decreased as the regeneration cycles increased. However, the performances of the PAM-PET cross-linked with different cross-linker are different. The *N*-halamine regeneration curve of PAM-PET-E presents a continuous drop of active chlorine till the 13th cycle where there is almost no active chlorine on the fabric. The regenerability evolutions of both PAM-PET-M and PAM-PET-D samples look similar and can be divided into three stages based on the curve shapes. In the first several regeneration cycles, both samples show abrupt drop of active chlorine contents. Following that drop, there is a "pseudo" stable stage. Surprisingly, there is another decrease after the first stable stage. Then, there is a more or less stable stage followed by another drop, which is relatively less steep. Finally, the active chlorine stays constant on both samples.

Mechanisms for the loss of regenerability

To find out the reasons for the degradation of *N*-halamine regenerability, FTIR, nitrogen content analysis, and acid group titration of the modified PET samples were used in this study. Figure 3 presents the subtracted FTIR spectrum (a) between PAM-PET-M after two regeneration cycles and PET pristine. After two regeneration cycles, besides the amide peak (1653 cm^{-1}), a new peak at 1700 cm^{-1} attributed to carboxylic acid occurs in the subtracted FTIR spectrum, suggesting hydrolysis of the immobilized PAM. This is the reason for the steep drop of active chlorine concentration on PAM-PET-M after the first several regeneration cycles. Because the pH of the chlorination solution is 11.4, alkaline

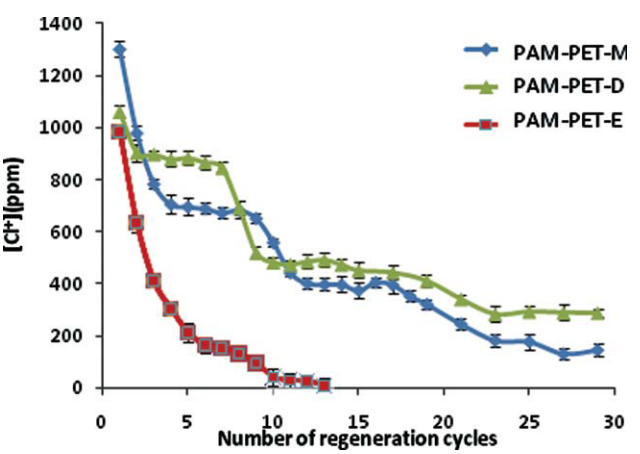

Figure 2 The active chlorine concentration [Cl^+] on PAM-PET versus number of regeneration cycles. [Color figure can be viewed in the online issue, which is available at wileyonlinelibrary.com.]

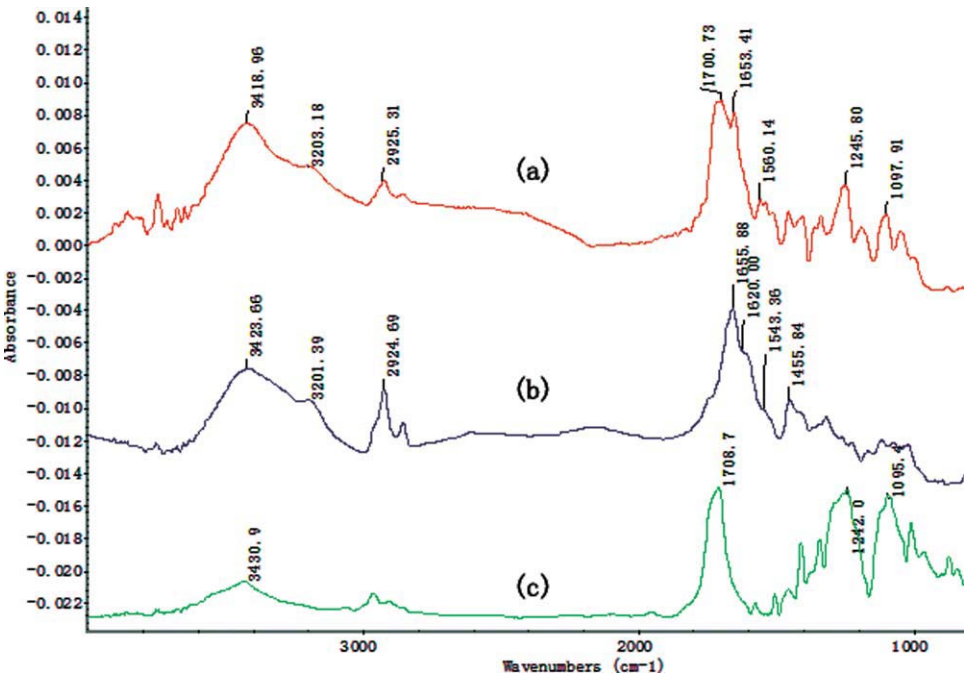

Figure 3 Subtracted FTIR spectra of (a) PAM-PET-M after two regeneration cycles and pristine PET, (b) PAM-PET-M with 0 regeneration cycles and pristine PET, and (c) FTIR spectra of PET pristine. [Color figure can be viewed in the online issue, which is available at wileyonlinelibrary.com.]

hydrolysis of the immobilized amide structure to carboxylic acid could occur during the chlorination, leading to loss of chlorine binding sites on PAM-PET. According to previous studies,[32,33] alkaline hydrolysis of PAM proceeds even at a higher rate compared with low-molecular-weight amides because the carboxylate groups formed in hydrolysis accelerate the hydrolysis of the neighboring amide groups (anchimeric contribution).

The finding that the amide structure was partially hydrolyzed into carboxylic acid during chlorination is also evidenced by the increase in carboxylic acid group quantity on fabric as shown in Table III. Carboxylic acid group on PET fabrics was quantified by a dye titration method.[34] Briefly, PET fabrics were allowed to interact with thionine acetate in its aqueous solution for 10 hr. The amount of thionite acetate that was adsorbed onto the surface of PET fabrics via ionic bonding with carboxylic acid can be calculated based on the concentration difference of thionine acetate before and after the adsorption. The amount of carboxylic acid group on pristine PET is 20.0×10^{-7} mol/g. After two regeneration cycles, the number increases to 88.5×10^{-7} mol/g for PAM-PET-M and to 61.3×10^{-7} mol/g for PAM-PET-D. Because nitrogen element only exists in the immobilized polymer network, nitrogen content can give an insight of the remaining IPN on PET. For PAM-PET-M, after two regeneration cycles, the lost nitrogen amounts to 90.9×10^{-7} mol/g [$(185.4–94.5) \times 10^{-7}$ mol/g]. The increased carboxylic acid group equals to 67.4×10^{-7} mol/g [$(88.5–21.0) \times 10^{-7}$ mol/g], which is around 74.3% of the amount of lost nitrogen (or amide structure). It means that around 25% of the nitrogen loss is due to the loss of IPN. This is because the cross-linker MBA also experiences hydrolysis during the chlorination, leading to the damage of the interlocking structure as shown in Scheme 2. However, applying the same analysis on PAM-PET-D, it was found that 92.7% of amide structure loss is due to hydrolysis of PAM amide and only around 7% was due to the loss of IPN. The much less amount of IPN damage in the case of PAM-PET-D is reasonable because the cross-linker DVB is nonhydrolyzable. Because the ester bond in the cross-linker EGDA is more susceptible to alkaline hydrolysis compared with the amide bond in MBA, more severe loss of the IPN occurs (Fig. 2) causing a quick decrease in active chlorine content with increase of the regeneration cycle.

Nitrogen contents of both PAM-PET-M and PAM-PET-D were plotted against regeneration cycles in Figure 4 to present a clearer view of the trend of change. As can be seen, the slope of amide structure loss decreases from second to 23rd cycle for both samples. During these regeneration cycles, the electrostatic repulsion between the OH— ions and the accumulating carboxylate anions (—COO^-) will decelerate the hydrolysis of amide. Even though there is a continuous decrease in nitrogen contents between second and seventh cycles for PAM-PET-D and fourth and eighth cycles for PAM-PET-M,

TABLE III
Contents of Functional Groups, Including [Active Chlorine], [Amide Group] and [Acid Group] on PAM-PET-M, PAM-PET-D, and PAM-PET-E Fabrics after Different Regeneration Cycles

Regeneration cycles	PAM-PET-M [Cl] (ppm)	[Amide group] (N analysis), 1×10^{-7} mol/g	[Acid groups] on fabric, 1×10^{-7} mol/g	PAM-PET-D [Cl] (ppm)	[Amide group] (N analysis), 1×10^{-7} mol/g	[Acid groups] on fabric, 1×10^{-7} mol/g	PAM-PET-E [Cl] (ppm)	Pristine PET [acid groups], 1×10^{-7} mol/g
0	0	185.4	21.0	0	186.5	20.6	0	20.0
1	1302 ± 30.2	168.8	–	1061 ± 24.9	–	–	984 ± 20.4	30.6
2	980 ± 24.9	94.5	88.5	904 ± 32.1	140.6	61.3	634 ± 33.2	20.9
3	784 ± 19.78	–	–	898 ± 14.8	–	–	412 ± 27.3	–
4	706 ± 26.7	–	–	879 ± 30.6	–	–	305 ± 24.9	–
5	696 ± 32.8	–	–	884 ± 25.5	109.2	33.3	214 ± 35.9	–
6	689 ± 21.2	74.5	28.08	867 ± 27.6	–	–	164 ± 30.7	20.2
7	674 ± 20.5	–	–	847 ± 21.4	–	–	154 ± 28.3	–
8	683 ± 33.1	–	–	692 ± 29.4	74.5	27.8	132 ± 27.8	–
9	652 ± 20.5	–	–	520 ± 23.8	–	–	96 ± 22.6	–
10	559 ± 15.1	–	–	483 ± 19.3	–	–	42 ± 31.1	–
11	443 ± 22.1	–	–	475 ± 26.8	–	–	30 ± 25.9	–
12	402 ± 21.4	–	26.56	486 ± 31.1	–	–	26 ± 28	20.2
13	398 ± 22.7	–	–	492 ± 27.6	51.1	30.8	10 ± 26.2	–
14	397 ± 30.4	–	–	474 ± 22.9	–	–	–	–
15	375 ± 29.6	–	–	452 ± 25.4	–	–	–	–
16	406 ± 17	–	–	–	–	–	–	–
17	397 ± 36.1	32.1	–	444 ± 28.4	–	–	–	–
18	354 ± 22.6	–	–	–	–	–	–	–
19	322 ± 19.1	–	–	412 ± 30.1	42.7	32.8	–	–
21	246 ± 22.3	–	–	342 ± 22.9	–	–	–	–
23	183 ± 24.2	12.2	21.68	284 ± 22.7	37.9	35.6	–	20.5
25	178 ± 31.5	–	–	294 ± 30.1	–	–	–	–
27	132 ± 19.9	–	–	301 ± 28.4	–	–	–	–
29	146 ± 24.4	14.5	21.4	289 ± 29.7	41.8	32.0	–	20.7

The IP based on weight of PAM-PET-M, PAM-PET-D, and PAM-PET-E are 13.17%, 13.25%, and 13.21%, respectively.

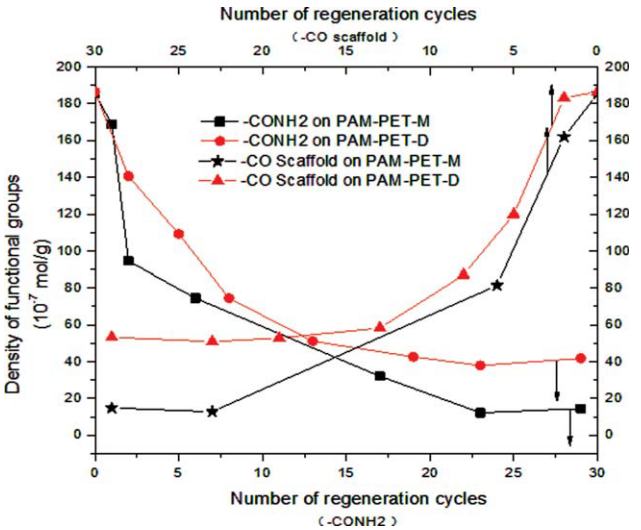

Figure 4 Amide content and C=O scaffold structure of PAM on PAM-PET as a function of the number of regeneration cycles. The density of —CH_2—CH(CO)— scaffold structure on PAM-PET equals the sum of densities of —$CONH_2$ (calculated from N content) and —COOH on hydrolyzed PAM network as shown in Table III. [Color figure can be viewed in the online issue, which is available at wileyonlinelibrary.com.]

amounts of *N*-halamine structure (equivalent to [Cl^+]) keep essentially constant (Fig. 2). Take PAM-PET-D for example, in second to sixth regeneration cycles, the loss of amide structure is due majorly to the loss of the immobilized IPN because the decrease in nitrogen content (from 140.6 to 109.2 $\times$ 10^{-7} mol/g) is accompanied by a simultaneous decrease in carboxylic acid group (from 61.3 to 33.3 $\times$ 10^{-7} mol/g). Peeling of the outermost immobilized PAM network exposes another layer PAM for chlorination, giving a pseudo stable active chlorine content ([Cl^+]).

However, loss of the immobilized IPN structure in the case of PAM-PET-D seems quite contradictory to the fact that DVB is nonhydrolyzable in the alkaline chlorination. Thus, surface carboxylic acid group of pristine PET was also analyzed by dye titration after it went through the same chlorination–quench cycles. As can be seen from the last column in Table III, carboxylic acid group slightly increases after the first chlorination and then decreases, indicating break down and dissolution of the PET polymer chain from the surface PET fabric. In the case of PAM-PET-D, because of the protection of the PAM network in the surface of modified PET, the hydrolysis of PET substrate primarily started after several regeneration cycles. The damage of surface PET resulted in the unlocking and loss of the immobilized PAM network. This explains the loss of PAM network in PAM-PET-D.

To better understand the status of the PAM network on PAM-PET, the contents of —$CONH_2$ and —COOH on PAM backbone can be added up to represent the content of total C=O or the CH_2—CH(CO)— scaffold structure. The data are presented in Figure 4. After 13 regeneration cycles, there is almost no loss of PAM network on PAM-PET-D although very small decrease in active chlorine concentration occurs because of further hydrolysis of amide. Nitrogen content and active chlorine value of both PAM-PET-D and PAM-PET-M keep essentially constant in the end as shown in Figures 2 and 4. This is consistent with the previous finding that hydrolysis of PAM results in BAB (B: —COOH and A: —$CONH_2$)-type structure and the formed carboxyl group can repel OH^- ions contributing to the stability toward further hydrolysis.[32,35] Also, after the initial hydrolysis of surface PET polymer in amorphous area, there is no further hydrolysis of PET under the mild hydrolytic condition (room temperature and pH 11) as can be seen from the date in Table III (the last column).

Summary of the impact of cross-linkers on the *N*-halamine regenerability

As presented in Figure 4, the content of total C=O or the CH_2—CH(CO)— scaffold structure on PAM-PET-D fabric after the first two regeneration cycles decreases only 2.79%, which means that almost all of the —CH_2—CH(CO)— scaffolds are retained on PAM-PET-D after the first two cycles. However, the network loss on PAM-PET-M samples is 12.6%, much bigger than that of PAM-PET-D. The scaffold structure of PAM-PET-D becomes stable after 13 cycles, whereas PAM-PET-M does not stabilize until 23 cycles. After 30 regeneration cycles, the quantity of active chlorine on PAM-PET-D is almost two times of that on PAM-PET-M, and the residual —CH_2—CH—C(O)— scaffold structure on PAM-PET-M is about three times of that on PAM-PET-M sample. In the end, there is almost no acid groups left on PAM-PET-M sample, but there is still 7.1 $\times$ 10^{-6} mol/g on PAM-PET-D sample. Both the structure durability and final active chlorine concentration are better with cross-linker DVB. In the end, the antibacterial regenerability of PAM-PET can be improved with DVB because active chlorine concentrations (the amount of *N*-halamine structure) are closely related to antibacterial activities. This will be discussed in the following section.

The relationship between active chlorine and antibacterial performance

N-halamine has favorable broad-spectrum antibacterial activities. The previous study has reported the antibacterial performance of *N*-halamine structure converted from PAM-immobilized PET (PAM-PET-

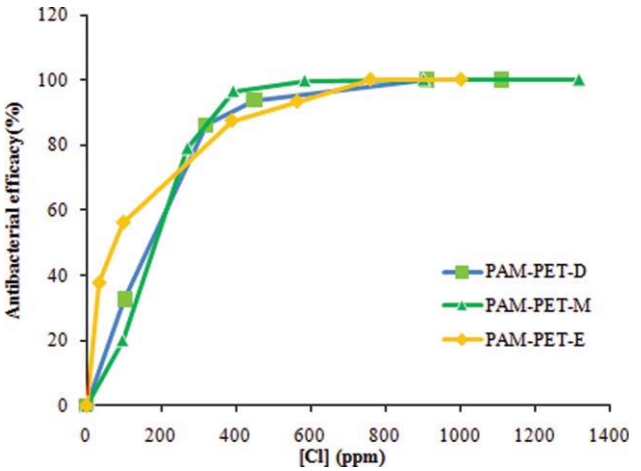

Figure 5 The relationship between antibacterial efficacy and active chlorine concentration on PAM-PET. The IP of PAM-PET-M, PAM-PET-D, and PAM-PET-E fabrics were 13.3% ± 1.4%, 12.9% ± 1.52%, and 13.2% ± 1.62%, respectively. [Color figure can be viewed in the online issue, which is available at www.wileyonlinelibrary.com.]

M, [Cl^+]: 1403 ppm) against an antibiotic-resistant clinical isolate of hospital-associated methicillin-resistant *S. aureus* (HA-MRSA isolate #70527) following the modified AATCC test method 100–2004.[18] The amide was converted to *N*-halamine in a chlorination process. The active chlorine on PAM-PET can be adjusted by the available chlorine concentration and chlorination duration in the chlorination process. By studying the relationship between active chlorine and antibacterial activity, regenerability of the antibacterial activity on PAM-PET can be inferred.

In this study, the chlorinated PAM-PET-M, PAM-PET-D, and PAM-PET-E samples (all with IP close to 13%) were all challenged by a HA-MRSA (isolate # 70527) following the modified AATCC test method 100-2004. The antibacterial activity of PAM-PET versus varying active chlorine concentrations was studied. The [Cl^+] value was adjusted by changing the available chlorine concentration of the chlorination solution. Five minutes of ultrasonic shaking was applied after the quench of the antimicrobial agent active chlorine to sufficiently release the bacteria attached on the fabric. Afterward, the samples providing total eradication of bacteria were investigated with an agar incubation test to further confirm total kill.

Figure 5 presents the relationship between antibacterial activity and active chlorine quantity on PAM-PET-M, PAM-PET-D, and PAM-PET-E. The kill ratio of the *N*-halamine increased with increasing biocidal stress ([Cl^+]). Because the initial bacterial quantity challenged by the modified fabric is definite, the kill ratio in established time represents the relative inactivation rate of the *N*-halamine structure. Thus, the trend indicates that the inactivation rate keeps increasing as *N*-halamine concentration raises.

All the PAM-PET-M, PAM-PET-D, and PAM-PET-E samples showed efficient antibacterial performance. No bacterial colonies could be observed even after 48 hr of culture on any agar plates contacted with PAM-PET-M and PAM-PET-D samples, which suggests total bacterial killing after the antibacterial test. This proves that antibacterial activity results of PAM-PET-M and PAM-PET-D are credible, and the total kill is a "real and true" finding. However, in the case of PAM-PET-E, several colonies were observed on the agar plate after 48 hr of incubation. This indicates that the antibacterial activity of PAM-PET-E samples was overestimated in Figure 5. This is due to the quick swelling of the PAM-PET-E fabric, and the 5-min ultrasonic shaking could not adequately extract the absorbed bacteria out of the PAM-PET-E fabric. The swelling ratio of PAM-PET-E is much higher than that of the other two PAM-PET-M and PAM-PET-D as shown in Table IV. It could carry out rapid absorption of bacterial solution and trapped the live bacteria in the PAM network. This is also why the PAM-PET-E samples demonstrate nominally "better" antibacterial efficacies than the other two samples when the active chlorine concentration is smaller than 300 ppm (Fig. 5). Thus, the results of the PAM-PET-E sample should be discounted. The following discussion will primarily focus on antibacterial activities of PAM-PET-M and PAM-PET-D samples.

As shown in Figure 5, concentration of *N*-halamine on PAM-PET affects the lethal activity

TABLE IV
The Swelling Ratio of PAM-PET with Different Cross-linkers

Sample[a]	PET	PAM-PET-M	PAM-PET-D	PAM-PET-E
Swelling ratio[b]	1.15 ± 0.01	1.30 ± 0.02	1.31 ± 0.02	1.49 ± 0.01
Swelling ratio of the grafted PAM network	–	2.41 ± 0.23	2.49 ± 0.24	4.01 ± 0.12

[a] AM concentration 3 mol/L and BP 0.055 mol /L. Cross-linker/monomer ratio of MBA/AM 1.5%, DVB/AM 1.1%, and EGDA 5%. The IP of the three samples are at 13.45% ± 0.5%.
[b] Swelling duration: 1 hr.

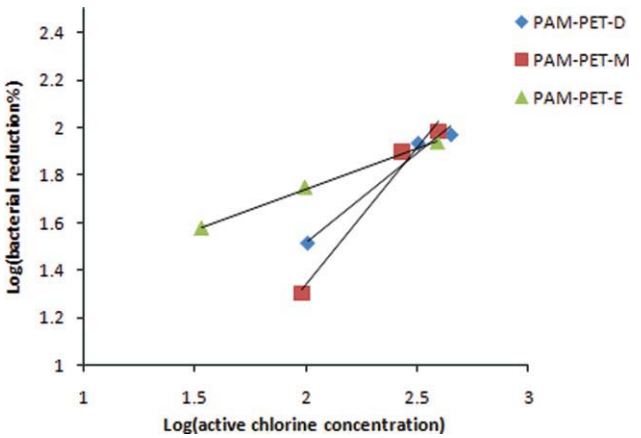

Figure 6 Log of bacterial reduction percentage versus log of concentration of antibacterial agent active chlorine [Cl^+]. [Color figure can be viewed in the online issue, which is available at www.wileyonlinelibrary.com.]

significantly. The relationship between the logarithm of bacterial reduction percentage in 10 min and active chlorine concentration is plotted in Figure 6. Russell has reported that the concentration of the biocide and respective time needed for the certain degree of inactivation follows[36]:

$$C_1^{\eta} t_1 = C_2^{\eta} t_2$$

The concentration exponent η is the measure of the effect of the changes in biocide concentration on cell death rate.

$$\eta = (\log t_2 - \log t_1)/(\log C_2 - \log C_1) \qquad (7)$$

In Figure 6, the logarithm of bacterial reduction and active chlorine concentration show a good linear relationship. The slope equals to the concentration exponent of *N*-halamine. As can be seen from Figure 6, the η values of chlorinated PAM-PET fabrics are all smaller than 2. It was reported that those biocides with η values smaller than 2 interacted with their target by chemical or ionic binding.[37] This result confirms that *N*-halamine functions as an oxidizing agent in destroying the cellular activity of protein.[38–41] The smaller η value as compared with various other biocides such as aliphatic and aromatic alcohols, phenolics, and sorbic acid[37] means that the antibacterial activity of the *N*-halamine is less dependent on its concentration. This enables *N*-halamine-modified PET to maintain an effective antibacterial activity even after many regeneration cycles.

As reported, effective biocidal action needs contact interaction of biocides with the target site and accumulation of the biocides to the damage level.[42] Thus, on the typical line of percent loss of bacterial viability versus applied biocidal stress, there is a initiation stage when the bactericidal effect is reversible because of the insufficient biocidal concentration.[43] However, this stage was not obviously shown in Figure 5. After the initiation stage, the biocidal effect of antibacterial agents such as *N*-halamine, which have an effect on metabolic activity could be supplemented by a autocidal activity resulted by the free radical accumulation through metabolic imbalance.[44] The autocidal effect leads to self-destruction of bacteria and accounts for the significant proportion of population death and the autoacceleration phenomenon in the second stage as shown in Figure 5 before total kill. It initiates the transition of sublethal damage of bacteria to cell death. Finally, irreversible total bactericidal effect is caused by high biocidal concentration. The characteristics of the first two stages could be influenced by the physicochemistry of *N*-halamine because the biocide physicochemistry could affect the efficacy of target interaction. Thus, besides chemical properties, both the steric hindrance of *N*-halamine monomer and network structure of immobilized modification network can significantly influence the accessibility of the biocide to the bacterial cell. This will be studied in future work.

The antibacterial regenerability

The antibacterial regenerability of PAM-PET fabrics after different regeneration cycles could be inferred by correlating their active chlorine concentration (Table III) with antibacterial activities according to the curves in Figure 5. It is showed that PAM-PET-M could provide a total kill of 10^6 CFU/mL HA-MRSA within 10 min after the second regeneration cycle ([Cl^+] = 980 ppm) and >99.7% reduction after the ninth regeneration cycle ([Cl^+] = 652 ppm). Also, the effective total inactivation activity of HA-MRSA by PAM-PET-D could sustain seven regeneration cycles ([Cl^+] = 847 ppm). However, PAM-PET-M after 29 regeneration cycles with 123 ± 32 ppm active chlorine can only inactivate 20.1% of the bacterium in 10 min. In the case of PAM-PET-D, even after 29 regeneration cycles, 306 ± 20 ppm active chlorine remaining on the sample can provide 86% kill of 10^6 CFU/mL HA-MRSA in 10 min and 100% kill in 20 min (datum is not included in Fig. 5).

CONCLUSIONS

Chemically inert PET fabrics were modified by forming surface thermoplastic semi-IPN with cross-linked PAM. The PAM-modified PET can be converted to effective biocidal *N*-halamine by chlorination. Analysis of the regenerability of *N*-halamine structure on PAM-PET-M, PAM-PET-D, and PAM-PET-E during 29 "titration–chlorination–regeneration" cycles shows

that the degradation of regenerability is due to hydrolysis of PAM, cross-linking points of PAM network, and PET during the chlorination process. The types of cross-linker influence the regenerability significantly. When DVB was used as the cross-linker, the modified fabric showed significantly better antibacterial regenerability. Even after seven regeneration cycles, PAM-PET-D samples demonstrated complete bacterial eradication within 10 min. A 100% reduction of 10^6 CFU/mL HA-MRSA could be attained within 20 min contact with the PAM-PET-D samples going through 29 regeneration cycles, where stabilization of the immobilized PAM structure has been achieved.

The authors are grateful for the financial support from the Natural Sciences and Engineering Research Council of Canada (NSERC) Discovery grant, the Manitoba Health Research Council (MHRC) Establishment grant, the Manitoba Medical Science Foundation (MMSF) grant, and the start-up fund from University of Manitoba.

References

1. Diaz, L. F.; Eggerth, L. L.; Enkhtsetseg, S. H.; Savag, G. M. Waste Manag 2008, 28, 1219.
2. Sabour, M. R.; Mohamedifard, A.; Kamalan, H. Waste Manag 2007, 27, 584.
3. Hamoda, H. M.; El-Tomi, H. N.; Bahman, Q. Y. J Environ Sci Health A Tox Hazard Subst Environ Eng 2005, 40, 467.
4. Altin, S.; Altin, A.; Elevli, B.; Cerit O. Pol J Environ Stud 2003, 12, 251.
5. Aizenshtein, E. M. Fibre Chem 2007, 39, 355.
6. Yang, S. C.; Kim, J. P. J Appl Polym Sci 2008, 108, 2297.
7. Neely, A. N.; Maley, M. P. J Clin Microbiol 2000, 38, 724.
8. Neely, A. N. J Burn Care Rehabil 2000, 21, 523.
9. Neely, A. N.; Orloff, M. M. J Clin Microbiol 2001, 39, 3360.
10. Gabbay, J.; Borkow, G. J Ind Text 2006, 35, 323.
11. East, A. J. In Polyester Fibers; Mclntyre, J. E., Ed.; Woodhead Publishing: Cambridge, 2005.
12. Ren, X.; Kocer, H. B.; Kou, L.; Worley, S. D.; Broughton, R. M.; Tzou, Y. M.; Huang, T. S. J Appl Polym Sci 2008, 109, 2756.
13. Chou, P. T.; Cao, G. J Sol-Gel Sci Technol 2003, 27, 31.
14. Rochery, M.; Vroman, I.; Campagne, C. J Ind Text 2006, 35, 227.
15. Louati, M.; Elachari, A.; Ghenaim, A.; Caze, C. Text Res J 1999, 69, 381.
16. Cireli, A.; Kutlu, B.; Mutlu, M. J Appl Polym Sci 2007, 104, 2318.
17. Song, Y. W. J Adhes Sci Technol 2006, 20, 1357.
18. Liu, S.; Zhao, N.; Rudenja, S. Macromol Chem Phys 2009, 211, 286.
19. Rudenja, S.; Zhao, N.; Liu, S. Eur Polym J 2010, 46, 2078.
20. Worley, S. D.; Williams, D. E. Crit Rev Environ Control 1998, 18, 133.
21. Sun, Y. Y.; Chen, T.; Worley, S. D.; Sun, G. J Polym Sci Part A: Polym Chem 2001, 39, 3073.
22. Sun, G.; Xu, X.; Bickert, J. R.; Williams, J. F. Ind Eng Chem Res 2001, 40, 1016.
23. Liu, S.; Sun, G. Polymer 2008, 49, 5225.
24. Sun, G. Durable and Regenerable Antimicrobial Textiles; American Chemical Society: Washington, DC, 2001.
25. Bender, W.; Peter, S. Antimicrobials for Synthetic Fibers; American Chemical Society: Washington, DC, 2001.
26. Kenawy, E.; Worley, S. D.; Broughton, R. Biomacromolecules 2007, 8, 1359.
27. Baselga, J.; Llorente, M. A.; Hernandez-Fuentes, I.; Pierola, I. F. Eur Polym J 1989, 25, 477.
28. Zhong, X. D.; Ishifune, M.; Yamashita, N. J Macromol Sci Pure Appl Chem 2000, 37, 49.
29. Arriola, D. J.; Cutié, S. S.; Henton, D. E.; Powell, C.; Smith, P. B. J Appl Polym Sci 1997, 63, 439.
30. Pascal, P.; Winnik, M. A. Macromolecules 1993, 26, 4572.
31. Barner-Kowollik, C.; Vana, P.; Davis, T. P. The Kinetics of Free-Radical Polymerization; Wiley-Interscience: Hoboken, NJ, 2002.
32. Kurenkov, V. F.; Hartan, H.-G.; Lobanov, F. I. Russ J Appl Chem 2001, 74, 543.
33. Nagase, K.; Sakaguchi, K. J Polym Sci Part A: Polym Chem 2003, 3, 2475.
34. Ivanov, V. B.; Behnisch, J.; Holländer, A.; Mehdorn, F.; Zimmermann, H. Surf Interface Anal 1996, 24, 257.
35. Liu, S.; Sun, G. J Appl Polym Sci 2008, 108, 3480.
36. Russell, A. D. In Russell, Hugo & Ayliffe' Principles and Practice of Disinfection, Preservation & Sterilization, Fraise, A.; Lambert, P. A.; Maillard, J.-Y., Ed.; Wiley-Blackwell: New York, 2004; Chap. 3.
37. Hugo, W. B.; Denyer, S. P. The Concentration Exponent of Disinfectants and Preservatives (Biocides); Blackwell Scientific Publications: Oxford, 1987.
38. Bloomfield, S. F. Handbook of Disinfectants and Antiseptics; Marcel Dekker: New York, 1996.
39. Dennis, W. H.; Olivieri, V. P.; Kruse, C. W. Water Res 1979, 13, 357.
40. Williams, D. E.; Swango, L. J.; Wilt, G. R.; Worley, S. D. Appl Environ Microbiol 1991, 57, 1121.
41. Williams, D. E.; Elder, E. D.; Worley, S. D. Appl Environ Microbiol 1988, 54, 2583.
42. Denyer, S. P. Int Biodeterior Biodegrad 1995, 36, 227.
43. Denyer, S. P.; Stewart, G. S. A. B. Int Biodeterior Biodegrad 1998, 41, 261.
44. Phillips-Jones, M. K.; Rhodes-Roberts, M. E. Studies of Inhibitors of Respiratory Electron Transport and Oxidative Phosphorylation; Academic Press: London, 1991.